LAWRENCE
LIVERMORE
NATIONAL
LABORATORY

UCRL-TR-207808

ALS Performance Summary - Update

A. M. Waters, W. D. Brown, H. E. Martz, Jr.

November 8, 2004

This work was performed under the auspices of the U.S. Department of Energy by University of California, Lawrence Livermore National Laboratory under Contract W-7405-Eng-48.

ALS Performance Summary – Update[1]

Amy M. Waters, William D. Brown and Harry E. Martz, Jr.
Lawrence Livermore National Laboratory,
Livermore, CA 94550

Introduction

High Energy Density Physics (HEDP) experiments play an important role in corroborating the improved physics codes that underlie LLNL's Stockpile Stewardship mission. Conducting these experiments, whether on the National Ignition Facility (NIF) or another national facility such as Omega, will require not only improvement in the diagnostics for measuring the experiment, but also detailed knowledge of the as-built target components and assemblies themselves. To assist in this effort, a defined set of well-known reference standards designed to represent a range of HEDP targets have been built and are being used to quantify the performance of different characterization techniques [*Hibbard, et al. 2004*]. Without the critical step of using reference standards for qualifying characterization tools there can be no verification of either commercial or internally-developed characterization techniques and thus an uncertainty in the input to the physics code models would exist.

Reference Standards

In FY03, two reference standards were fabricated and characterized using metrology tools. One of the reference standards was built with a cylindrical geometry and contained features similar to those on a Super Nova Raleigh Taylor (SNRT) target. The other reference standard was built with a spherical geometry and contained features similar to those on a double shell target. The standards were designed for manufacturability, stability and to provide a range of features that can be measured using NDE methods. For reference standard fabrication details and metrology results see [*Hibbard, et al. 2004*].

Digital Radiography System Performance

In an attempt to begin characterizing the reference standards, we have acquired data nondestructively using different x-ray digital radiography (DR) and computed tomography (CT) systems. Reports for the performance of each DR/CT system investigated and used to characterize these reference standards are given elsewhere [*Waters, et al. 2004, Waters, et al. 2004a, Gross, et al. 2004*]. Here we present the report on the tomography beamline 8.3.2 at the Advance Light Source (ALS) located at Lawrence Berkeley National Laboratory (LBNL).

The synchrotron source is a high flux, low divergence x-ray source capable of producing near monochromatic x-rays. The x-ray source is tunable for energies from 6 to 30 keV.

[1] *This work was performed under the auspices of the U.S. Department of Energy by University of California, Lawrence Livermore National Laboratory under Contract W-7405-Eng-48.*

The data presented here was acquired at 6 keV. The LLNL designed detector consists of a cadmium tungstate ($CdWO_4$) scintillator optically coupled to a 3088 X 2056 thermoelectrically cooled charged coupled device (CCD) camera with 12-bit dynamic range. The pixel size of the camera is 9 µm. The lens used by the system gives an optical magnification of 5.4X, which results in a pixel size of 1.67 µm at 1 X 1 binning[2]. To increase signal-to-noise ratio, all data was acquired with 2 X 2 binning, which results in an effective pixel size of 3.34 µm. The system also contains an *x, y, z* stage with theta rotation to manipulate the objects. Figure 1 is a picture of the detector and stages inside the ALS Tomography Beamline 8.3.2 hutch.

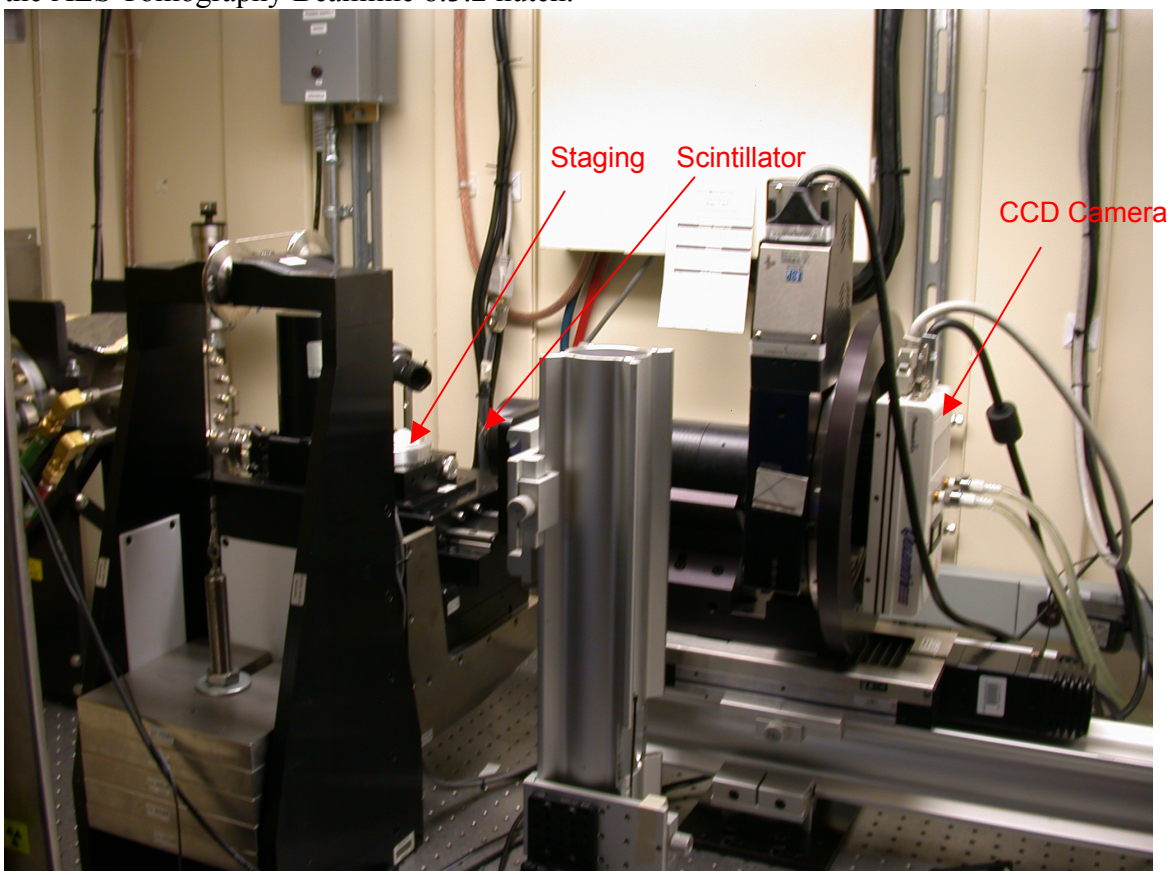

Figure 1. LLNL based detector and stages inside synchrotron beamline 8.3.2 hutch

For computed tomography, 360 projection images were acquired over 180 degrees. Each projection image was acquired for 4.5 seconds. Total CT data acquisition time was approximately 30 minutes.

In order to begin quantifying digital radiography system performance, a thin (0.51 mm) polished tantalum edge was imaged using identical DR/CT data acquisition parameters. Transmission images (I/I_0) were created and a 10-pixel wide one-dimensional lineout was taken from the polished edge to determine the edge response of the system. Two lineouts taken from different areas of the tantalum edge image are shown in Figure 2.

[2] *Because of the low divergence angle of the synchrotron source, the system is operated in parallel beam geometry and there is little or no geometric magnification of the object.*

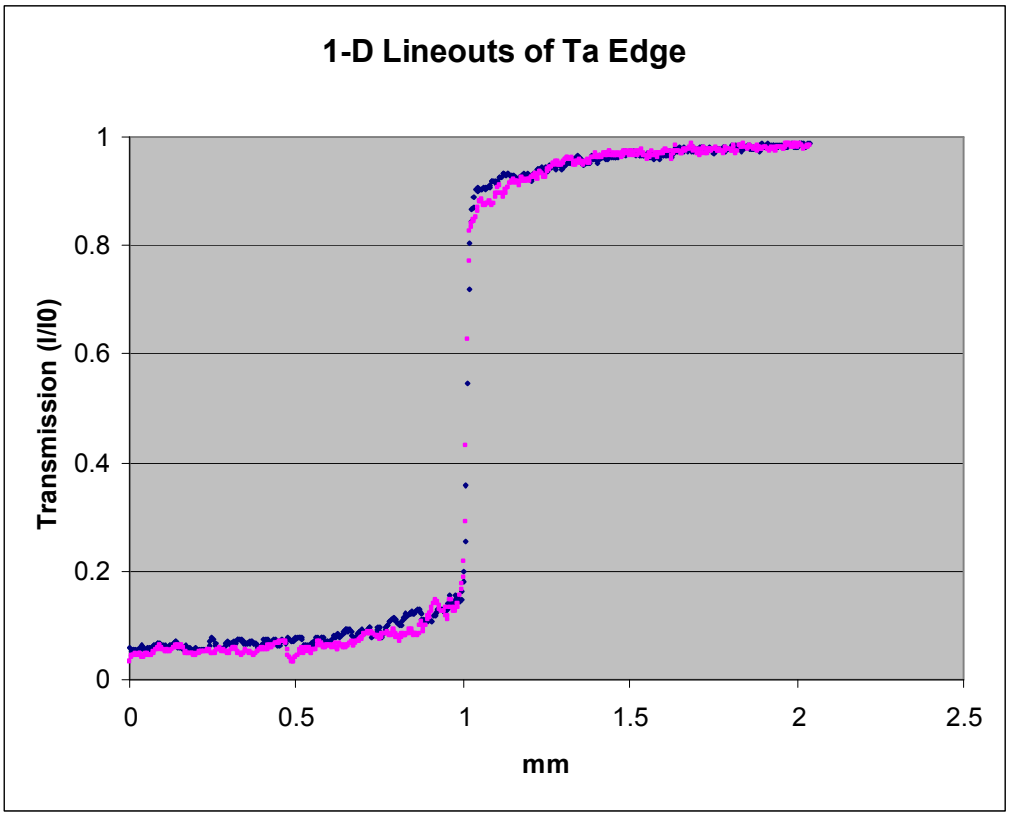

Figure 2. Two 10-pixel wide one-dimensional lineouts were taken from the thin tantalum edge transmission image. These lineouts were used to calculate the DR MTF's to demonstrate repeatability and DR performance.

The one-dimensional lineouts were used to measure the projection or DR Modulation Transfer Function (MTF) of the system. To calculate the MTF for the ALS Tomography Beamline, the derivative of the line-out (edge response) was calculated, resulting in what is called the edge-spread function. The Fourier transform of the edge-spread function is the line-spread MTF. The MTF is a frequency-domain description of the spatial resolution of an imaging system or component [*Hasegawa 1991, Logan, et al. 1998*]. The MTF of a system is the product of the MTFs of each of the components individually, and thus is a preferred technique for many imaging experts. The MTF of a system is usually presented as a graph with frequency in mm^{-1}, or linepairs per millimeter (lp/mm) on the horizontal, or x-axis. At low spatial frequencies, the MTF usually approaches 1. The MTF falls with increasing frequency, and can never exceed a sinc function [sin(x)/x], where x is the pixel size. DR MTFs for the ALS Tomography Beamline as a function of frequency in lp/mm is presented in Figure 3.

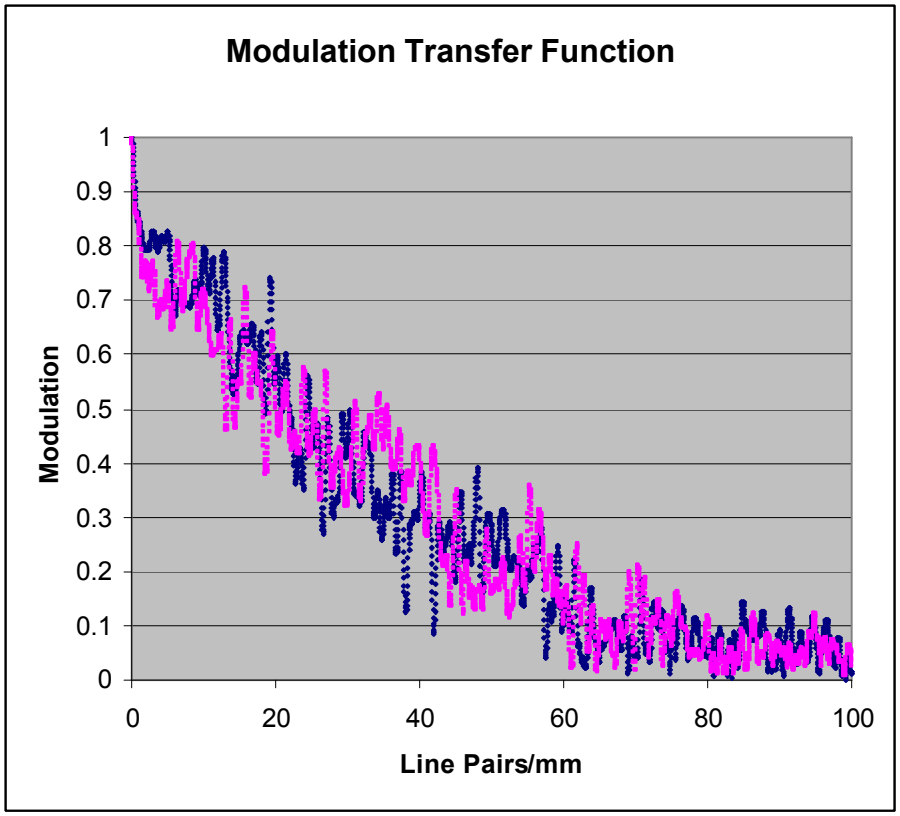

Figure 3. Two MTFs calculated for the ALS Tomography Beamline using the two lineouts shown in Figure 2. At 20 lp/mm, the modulation is ~50%.

To determine spatial resolution, one commonly used rule of thumb is to multiply the pixel size at the object by a factor of 2.5. Using this simple estimate of the spatial resolution for the parameters described above, the resulting resolution of the beamline DR data is approximately 8.35 μm. Another quick and easy way to get a sense of the spatial resolution of a system is to fit the edge-spread function (calculated as the derivative of the one-dimensional lineout) with a Gaussian. The resulting Full Width Half Maximum (FWHM) of the Gaussian can be multiplied by the pixel size at the object to give an indication of "worst-case" system resolution. For the beamline, the FWHM of the Gaussian-fit edge-spread function was calculated to be 3.9, indicating a worst-case system spatial resolution of approximately 13.0 μm.

Other techniques exist to quantify system performance, such as the Signal to Noise Ratio (SNR). The SNR is defined as the difference between the mean of two signals (in our case the two signals are within the Ta edge, and outside the Ta edge) divided by the square root of the sum of the squares of their respective standard deviations:

$$\frac{S_1 - S_2}{\sqrt{s_1^2 + s_2^2}},$$

where S is the mean of the signal and σ is the standard deviation of the signal.

The SNR of the DR of the tantalum edge can be calculated using the one-dimensional line-outs taken from the tantalum edge transmission image, and can also be calculated over an area (two-dimensions) (for both calculations S_1 is defined as the mean far from the Ta edge and S_2 is defined as the mean within the Ta edge). The two-dimensional DR SNR of the Ta edge was determined for an area of 150 X 150 pixels, and was calculated to be 58.7.

Several preprocessing steps were necessary before the DR projections could be reconstructed into a CT volume. Each projection image was first converted into ray sums, or attenuation radiographs [$\ln(I_0/I)$], and outlying pixels were removed using a median filter comparison algorithm. Attenuation is a function of material density, elemental composition, x-ray energy and path length through the material. Thus, in the resulting attenuation digital radiographs as displayed here, darker regions indicate lower attenuating materials and/or shorter path lengths, while lighter areas indicate higher attenuating materials and/or longer path lengths.

The attenuation radiograph of the spherical reference standard is shown in Figure 4 (left image). It is easy to see the air gap at the top surface of the carbonized resorcinol formaldehyde (CRF) as well as the air gap located at the bottom surface of the CRF near the step joint. Dark areas in the step joint indicate regions with less material which suggest that the step joint was not bonded completely. A faint line above the inner hemisphere indicates the presence of the 10-µm radius groove within the CRF [*Hibbard, et al. 2004*].

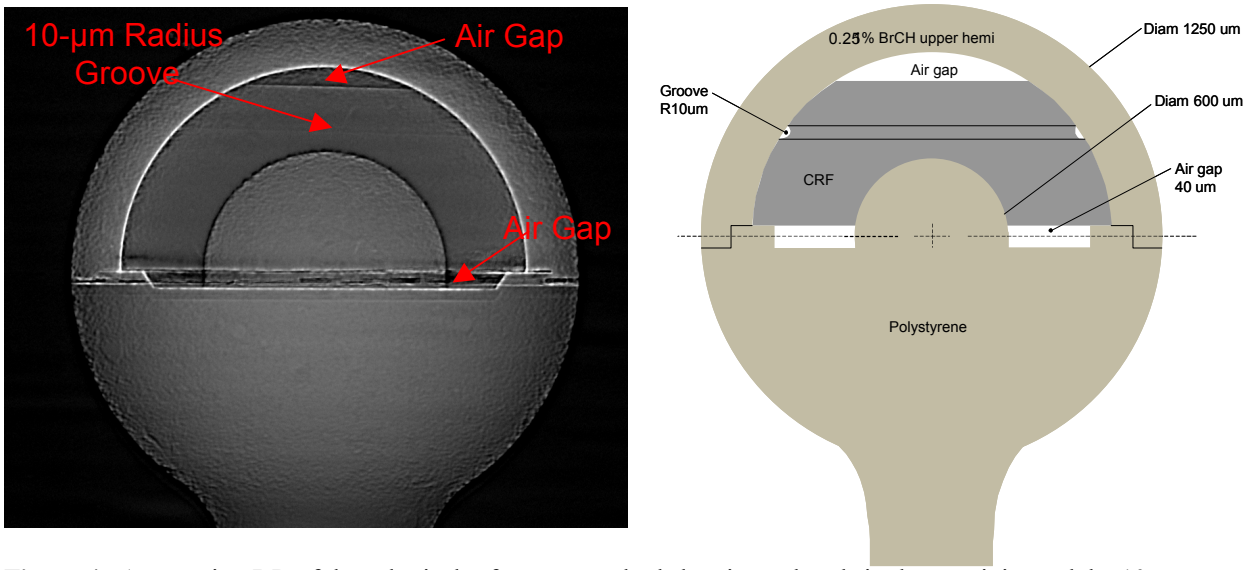

Figure 4. Attenuation DR of the spherical reference standard showing unbonds in the step joint and the 10-µm radius groove in the CRF (Left Image). Schematic of the spherical reference standard to compare with the DR results (Right Image).

Due to the nature of the synchrotron source, the flux of the synchrotron decreases over time. To compensate for this decrease, a new I_0 image was acquired every 20 projections. Figure 5 shows one of the ten I_0 images. This image reveals the imperfections in the $CdWO_4$ scintillator and is typical of the I_0 images. Because of the

scintillator imperfections, it is very difficult to normalize the I projection image by the I_0 image[3]. In Figure 4 (left image), the spherical reference standard appears to have surface roughness. However, this is due to the inability to acquire a good normalized attenuation image ($\ln I_0/I$) rather than surface roughness in the standard.

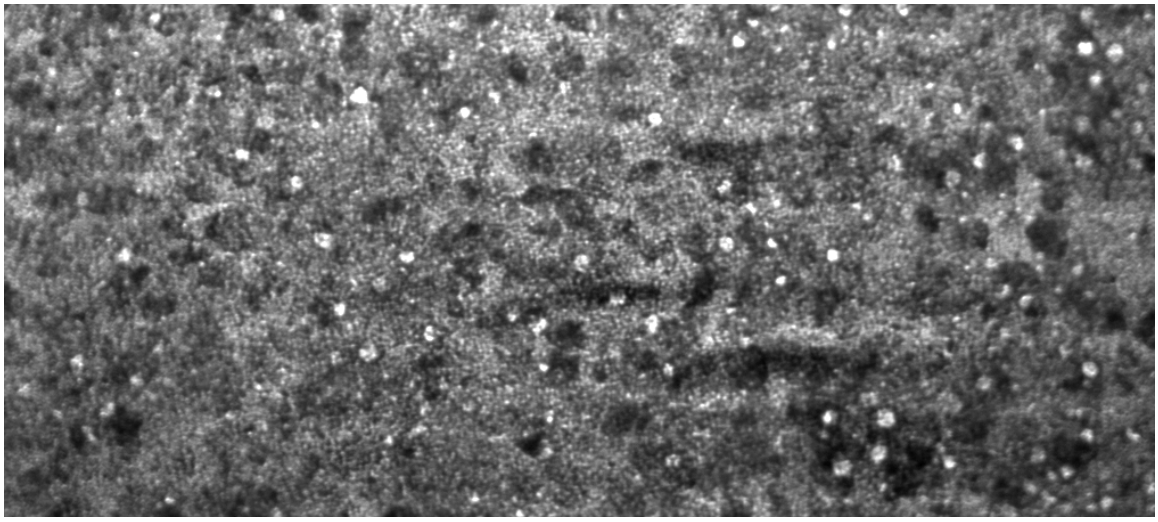

Figure 5. One of ten I_0 images acquired showing scintillator imperfections.

CT Data

The imperfections in the scintillator appear as detector imbalances in the sinograms. The true detector imbalances and the scintillator defects were normalized ($\ln I_0/I$) to minimize ring artifacts in the reconstructed image. A second step was performed with a ring removal algorithm on the sinograms to further reduce ring artifacts. Even after applying the ring removal algorithm, ring artifacts were not completely removed. Because of the low divergence angle of the synchrotron source, a simple parallel beam reconstruction was used to reconstruct the CT sliced data.

Many features of the spherical standard can be seen in the CT images provided in Figure 6. Figure 6 (left image) reveals a CT image of the step joint. In the step joint, many voids or unbonds (dark areas) can be seen. In the area above the step joint (right image), high attenuating material (bright areas) at 2 o'clock just inside the outer shell, possibly glue, has wicked into the CRF. Figure 7 is a CT image along the vertical axis of the spherical standard. This image is orthogonal to the images in Figure 6. The air gap can clearly be seen above the CRF in this image.

[3] *It should be noted that the normalization is accomplished for areas outside the part,* I_0*, but not inside the part, I, since the imperfections are non-linear.*

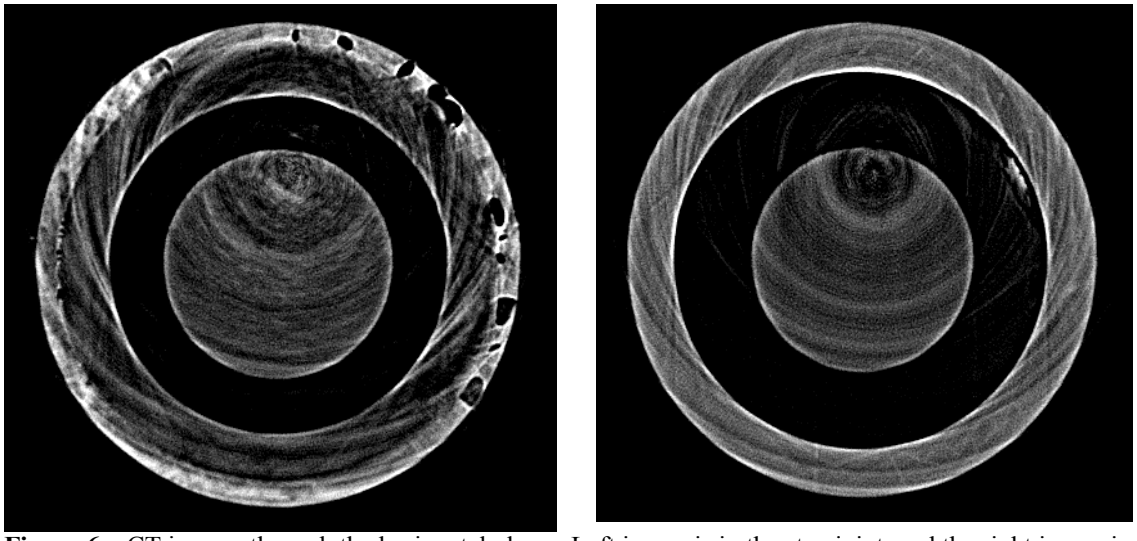

Figure 6. CT images through the horizontal plane. Left image is in the step joint, and the right image is just above the step joint. Note the ring artifacts in both images.

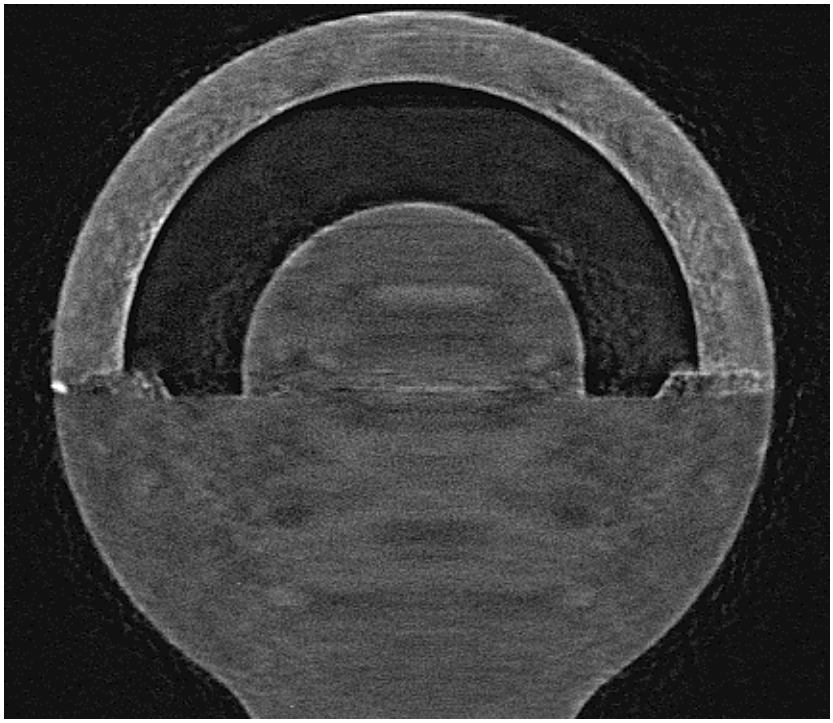

Figure 7. CT image of the vertical plane.

Summary

We have begun to quantitatively measure the ALS tomography beamline 8.3.2 digital radiography and computed tomography system performance. Tomography data has been acquired for the spherical standard. The ALS Tomography Beamline was just operational when the spherical standard data set was acquired. ALS personnel were still fine tuning the monochromator on the beamline and the LLNL detector was not

completely aligned to the beamline. Since this data was acquired, the synchrotron system has undergone upgrades to the scintillator and the synchrotron source. We have been unable to get beamline time since the acquisition of the spherical data set, and we should acquire new data to quantitatively measure the MTF and SNR after the upgrades.

Future Work

Much work needs to be done to quantify the CT data and qualitative observations described here. Any quantified data resulting from this project must be relevant to the target design and fabrication communities. To this end we are working with those groups to identify data of interest. The information that has been determined to be of interest for the spherical reference standard include: quantifying the 2-μm gap built into the outer half of the step joint, see Figure 4 (right image), in the spherical reference standard; determining if the inner step joint is completely joined; qualitatively identifying flaws such as voids, and the wicking of glue; determining distributions of identified flaws, including maximum volumes, total number, and volume fractions; measuring to 1 μm the concentricity of the outer hemishell and inner hemisphere; quantifying wall thicknesses, including the mean and standard deviations; measuring the volume of the air gap between the CRF and the BrCH upper hemisphere; and measuring the 10-μm radius groove in the CRF. Future efforts should include CT acquisition of cylindrical standard, CT acquisition of LDPE, Au and Cu rods and acquiring 3D rendering of standards.

References

Gross, J., B. Kozioziemski, A. Waters, and H. Martz, "APS Performance Summary – Update", Lawrence Livermore National Laboratory, Livermore, CA, UCRL-TR-207260 (2004).

Hasegawa, B., *The Physics of Medical X-ray imaging*, Madison, WI, Medical Physics Publishing, 1991.

Hibbard, R., M. Bono, A. Waters, and H. Martz, "TechBase Final Report for: Production and Documentation of Mesoscale Metrology and Characterization Reference Standards", Lawrence Livermore National Laboratory, Livermore, CA, *to be published* (2004).

Logan, C., J. Haskins, K. Morales, E. Updike, J. Fugina, T. Lavietes, D. Schneberk, G. Schmid, K. Springer, P. Soltani, and K. Swartz, "Evaluation of an Amorphous Selenium Array for Industrial X-Ray Imaging", Lawrence Livermore National Laboratory, Livermore, CA, UCRL-ID-132315 (1998).

Waters, A., H. Martz, C. Logan, J. Gross, and D. Chinn, "KCAT Performance Summary - Update", Lawrence Livermore National Laboratory, Livermore, CA, UCRL-TR-203519-REV-1 (2004).

Waters, A., H. Martz, D. Chinn, C. Logan, J. Gross, and D. Scott, "Xradia Performance Summary - Update", Lawrence Livermore National Laboratory, Livermore, CA, UCRL-TR- 206565 (2004a).